BIOCHEMISTRY
including biophysical chemistry & molecular biology

Article

pubs.acs.org/biochemistry

Altering the Activation Mechanism in *Thermomyces lanuginosus* Lipase

Jakob Skjold-Jørgensen,[†,‡] Jesper Vind,[‡] Allan Svendsen,[‡] and Morten J. Bjerrum*[,†]

[†]Department of Chemistry, University of Copenhagen, Universitetsparken 5, 2100 København Ø, Denmark
[‡]Novozymes A/S, Brudelysvej 35, DK-2880 Bagværd, Denmark

Supporting Information

ABSTRACT: It is shown by rational site-directed mutagenesis of the lid region in *Thermomyces lanuginosus* lipase that it is possible to generate lipase variants with attractive features, e.g., high lipase activity, fast activation at the lipid interface, ability to act on water-soluble substrates, and enhanced calcium independence. The rational design was based on the lid residue composition in *Aspergillus niger* ferulic acid esterase (FAEA). Five constructs included lipase variants containing the full FAEA lid, a FAEA-like lid, an intermediate lid of FAEA and TlL character, and the entire lid region from *Aspergillus terreus* lipase (AtL). To investigate an altered activation mechanism for each variant compared to that of TlL, a combination of activity- and spectroscopic-based measurements were applied. The engineered variant with a lid from AtL displayed interfacial activation comparable to that of TlL, whereas variants with FAEA lid character showed interfacial activation independence with pronounced activity toward pNP-acetate and pNP-butyrate below the critical micelle concentration. For variants with lipase and esterase character, lipase activity measurements further indicated a faster activation at the lipid interface. Relative to their activity toward pNP-ester substrates in calcium-rich buffer, all lid variants retained between 15 and 100% activity in buffer containing 5 mM EDTA whereas TlL activity was reduced to less than 2%, demonstrating the lid's central role in governing calcium dependency. For FAEA-like lid variants, accessible hydrophobic surface area measurements showed an approximate 10-fold increase in the level of binding of extrinsic fluorophores to the protein surface relative to that of TlL accompanied by a blue shift in emission indicative of an open lid in aqueous solution. Together, these studies report on the successful alteration of the activation mechanism in TlL by rational design creating novel lipases with new, intriguing functionalities.

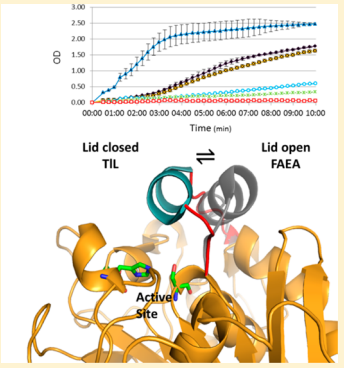

Lipases are triacylglycerol acylhydrolase enzymes (EC 3.1.1.3) that catalyze the hydrolysis of long chain acylglycerols at the water−lipid interface. The essential role of lipases in nature transcends into biotechnological applications, where they are used in the production of biopolymers and biodiesel, in the synthesis of fine chemicals, and as catalysts in detergents.[1] The *Thermomyces lanuginosus* lipase (TlL) is a single polypeptide chain consisting of 269 amino acids comprising eight parallel β-sheets surrounded by five interconnecting α-helices with three disulfide bonds (C22−C268, C36−C41, and C104−C107).[2] The organizational architecture of these secondary structures is common for proteins in the α/β-hydrolase family.[3] Furthermore, TlL contains a single glycosylation site at position Asn33 by *N*-acetylglucosamine, mannose, and galactose,[4] which has been shown to play an important role in the properties of binding to micelles.[5]

The catalytic triad in TlL, composed of residues Ser146, His258, and Asp201, is shielded from the external environment by a lid region composed of an α-helix with two hinge domains anterior and posterior to the lid.[2] Crystal structures of the TlL with its lid in a closed and open state have indicated that this lid plays a central role in the activation of the enzyme.[6,7] The TlL and most other lipases become fully activated upon binding to a water−lipid interface and remain virtually inactive when the substrate is in an aqueous solution in the absence of an interface,[8] a phenomenon termed "interfacial activation".[7] As the substrate reaches concentrations beyond its critical micelle concentration (CMC), the lipase activity increases more than 10-fold with a concomitant opening of the lid. Activity measurements[9,10] and MD simulations[11−13] on TlL and related lipases suggest that the opening of the lid is energetically unfavorable in aqueous solutions. This is supported by the fact that lid opening exposes a large hydrophobic patch representing ∼10% of the total surface area of the enzyme.[7] Also, the distinct distribution of hydrophobic amino acids in the lid of TlL indicates a favorable interaction with the active site in a hydrophilic environment keeping the lid closed. As the lipase encounters a lipid surface, the lid moves away from the active site and hydrophobic residues Ile, Trp, and Phe in the lid are proposed to penetrate the lipid layer to position the lipase correctly for catalysis at the interface.[14]

The FAEA is one of the most studied ferulic acid esterases.[15] Interestingly, the primary sequence of FAEA is only ∼30%

Received: February 24, 2014
Revised: May 26, 2014
Published: May 28, 2014

   dx.doi.org/10.1021/bi500233h | *Biochemistry* 2014, 53, 4152−4160

identical with that of TlL, but their tertiary structures are remarkably similar. Although the FAEA and TlL show similar architectural arrangements, the two enzymes have different activation functionalities.[16] The FAEA does not exhibit lipase activity,[17] and its activity is supposedly independent of an interface given the distribution of polar residues in its lid (residues 67−83), including an N-glycosylation site ("NYTL"). Therefore, to change the activation mechanism in TlL, a rational design approach was applied on the basis of the lid residue composition in FAEA, spanning 17 residues. The lid from AtL was included as a proof of concept demonstrating the impact of lid residue composition on lid activation. Previous studies[18,19] have investigated the impact of single-site mutations in the hinge domains of the lid region in *Aspergillus niger* lipase based on FAEA. Also, it has been shown that it is possible to adapt esterase activity and lower lipase activity by incorporating the entire lid region from FAEA to different lipase backbones.[20] In this work, we have created lid variants with a series of mutations in the lid region spanning both the hinge domains and the α-helix based on the lid residue composition in FAEA facilitating the generation of lipase variants with an intermediate lid composition. Variants 1L and 2L contained FAEA-like lids; variants 3L and 3C had intermediate lid compositions of both FAEA and TlL character, and variant 4L contained the entire lid domain from AtL. In this study, activity assays and spectroscopic methods were combined to elucidate the open−closed states of the lid in each variant *in vitro*. Activity on water-soluble pNP-acetate was determined for each variant, and the interfacial activation profile was studied by measuring the hydrolytic activity on pNP-butyrate below and above its critical micelle concentration. Lipase activity was determined by measuring the hydrolytic activity on pNP-decanoate embedded in a triolein layer. Hydrolytic activity on pNP-butyrate and -decanoate was also determined in the presence of Triton X-100 with and without calcium ions and EDTA. Finally, fluorescence spectroscopy was used to reveal differences in the Trp microenvironment and binding of extrinsic fluorophores to hydrophobic areas on the protein surface.

MATERIALS AND METHODS

Materials. Unless designated, all reagents and biochemical supplies were purchased from Sigma-Aldrich and affiliates.

Engineering of Lid Variants. Lid variants were created by rational design based on the lid regions from *A. niger* ferulic acid esterase (FAEA), *T. lanuginosus* lipase (TlL), and *Aspergillus terreus* lipase (AtL), spanning 17 residues. 1L contained the entire FAEA lid, and 2L contained a FAEA-like lid with three additional conservative mutations and with the "NYTL" glycosylation site removed. For the rational design of 3L and 3C, a PSI search[21] was conducted in the UniProtKB database using the FAEA primary sequence as a query [Protein Data Bank (PDB) entry 1UZA[15]]. The resulting FAEA-related esterase and lipase sequences were aligned using MUSCLE[22] and analyzed for specific reoccurring motifs in the posterior hinge domain, H2, of the lid region in ClustalX version 1.83[23] (Figure S1 of the Supporting Information). The "PQ" motif was found to be prevalent in a number of hydrolases from different species, e.g., *Parmelia omphalodes*, *Penicillium chrysogenum*, *Emericella nidulans*, *Aspergillus kawachii*, *Coccidioides posadasii*, *Coccidioides immitis*, *Penicillium marneffei*, *Talaromyces stipitatus*, *Setosphaeria turcica*, *Mycosphaerella graminicola*, and *Septoria musiva*, and was therefore incorporated into the lids of 3L and 3C. Other parts of the lid region contained residues from either TlL or FAEA. In addition, 3C was constructed with the intention of locking the lid in an open conformation with a disulfide bond. Variant 4L was made by adapting the entire lid domain from AtL. For alignment of entire protein sequences for lid variants and TlL, refer to Figure S2 of the Supporting Information.

Variant Construction, Transformation, and Screening. All variant genes were generated by spliced overlap extension (SOE) polymerase chain reaction (PCR)[24] with flanking primers 5′-AGAGCTTAAAGTATGTCCCTTG-3′ (forward) and 3′-CCCCATCCTTTAACTATAGCG-5′ (reverse) and hybrid primers (Table S1 of the Supporting Information). The lipase variant genes were inserted into a cloning plasmid containing the TlL gene, and purified DNA was sequenced across the whole gene, transformed into an *Aspergillus oryzae* strain, and fermented according to previous methods.[25] Protoplasts were stored at −80 °C and thawed when needed. Expression was verified by running sodium dodecyl sulfate−polyacrylamide gel electrophoresis (SDS−PAGE) analysis. Variant screening was conducted for successfully transformed *A. oryzae* strains using a standard pNP-valerate activity assay.[26]

Purification. Fermentation broths were sterile filtered using filter units (Nalgene) with appropriate filters (CAT model 1820-090, Whatman). NaCl was added to the filtered supernatant to a final concentration of 1 M. The protein purifications were conducted with an ÄKTA Prime instrument (Amersham Biosciences) according to a previously published protocol.[27] Variants were highly purified with no observable contamination verified by SDS−PAGE. All samples were buffer-exchanged and concentrated in 50 mM MOPS (pH 7.5) using centrifugal filter units (Ultracel-10K, Millipore). The intact molecular weight of each variant and TlL was verified by LC-ESI-TOF-MS analysis (Table S2 of the Supporting Information). Furthermore, as indicated by SDS-PAGE analysis, in-gel digest mass spectrometry confirmed glycosylation of the "NYTL" site in the lid of variant 1L (data not shown).

Circular Dichroism Spectroscopy. Circular dichroism (CD) spectroscopy was used to characterize and compare protein folding of TlL and lid variants in aqueous solutions in the absence of an interface. A J-815 CD spectrometer (Jasco) was used to record CD spectra. Spectra were recorded in 10 mM Tris buffer (pH 7.5), with protein concentrations of ∼0.4 mg/mL. Quartz glass cuvettes for far- and near-UV CD with light paths of 0.02 cm were used. CD spectra were collected from 260 to 178 nm with 1 nm intervals. A minimum of five scans were taken for each sample. The spectra were averaged, and blanks were subtracted. Finally, the spectra were converted to $\Delta\varepsilon$ per residue molar absorption units of CD (M^{-1} cm^{-1}) using the equation $\Delta\varepsilon = \theta(0.1 \times MRW)/(3298lc)$, where θ is machine units in millidegrees, MRW is the protein mean weight per residue in grams per mole, l is the path length in centimeters, and c is the protein concentration in milligrams per milliliter. Modeling of the CD spectra was conducted at http://dichroweb.cryst.bbk.ac.uk/html/home.shtml[28] using the CDSSTR algorithm with reference set 1 optimized for 178−260 nm for secondary structure analysis.[29]

Lipase Assay. Microtiter plates (96 wells, NUNC 269620) were coated with 100 nmol of triolein (CAS Registry No. 8001-25-0) and 100 nmol of pNP-decanoate (CAS Registry No. 1956-09-8). The stock solutions were made by dissolving the substrate in 95% hexane (CAS Registry No. 110-54-3) in blue cap flasks, making sure that the lid was tightly sealed to prevent

dx.doi.org/10.1021/bi500233h | *Biochemistry* 2014, 53, 4152−4160

evaporation. The plates were coated by transferring the substrate solutions to each well by a multipipette and letting the plates dry for 2 h in a flow hood with the light switched off (avoiding light oxidation of the pNP-substrate). The assay was conducted in 100 mM Tris and 1 mM $CaCl_2$ (pH 8, 9, or 10). Ten microliters of the enzyme solution was transferred to 190 μL of buffer on a separate 96-well microtiter plate; 150 μL of the enzyme dilution was transferred to the coated lipase assay plate with a multipipette (Liquidator RAININ, Mettler Toledo). The coated assay plate was immediately placed in the plate reader (SpectraMax Plus 384, Molecular Devices), and the increase in absorbance due to the *p*-nitrophenolate anion was measured at 405 nm. The assay was conducted at 25 °C for 10 min.

Interfacial Activation (IA) Assay. The IA assay was conducted according to the method described in ref 9, however, in a microtiter plate setup using nonbinding plates (Corning, catalog no. 3995) to minimize adsorption of lipase to the well surface and hence lower artificial activity levels. The substrate dilutions were emulsified by sonication for 2 min prior to the assay. The reaction was started by addition of an enzyme solution (10 μL) to 190 μL of a substrate solution. Hydrolysis of pNP-butyrate was monitored at 400 nm with a UV−vis spectrophotometer (SpectraMax Plus 384, Molecular Devices) at 25 °C.

pNP-Acetate Assay. Activity toward pNP-acetate was determined in 50 mM Mops (pH 7.5) at various substrate concentrations. A pH of 7.5 was chosen because of the lability of this substrate at alkaline pH. A stock solution was made in 2-propanol and diluted in buffer to reach appropriate substrate concentrations. A 10 μL lipase sample was added to each well of a 96-well microtiter plate. To minimize the adsorption of lipase to the well surface, nonbinding plates were used. With a multipipette (Liquidator, RAININ), 190 μL of the substrate solution was transferred to each well. The increase in absorbance was detected at 400 nm using a UV−vis spectrophotometer (SpectraMax Plus, Molecular Devices).

Hydrolysis of pNP-Esters. Hydrolytic activity toward pNP-ester substrates, pNP-butyrate and pNP-decanoate, was determined by conducting the assay in two different buffers: (a) 50 mM Tris, 10 mM $CaCl_2$, and 0.4% Triton X-100 and (b) 50 mM Tris, 5 mM EDTA, and 0.4% Triton X-100 (pH 7.5). pNP-ester substrates were dissolved in 2-propanol and diluted in the respective buffers. A 10 μL lipase sample was added to each well of a 96-well microtiter plate. With a multipipette (Liquidator, RAININ), 190 μL of the substrate solution was transferred to each well. The increase in absorbance was detected at 400 nm using a UV−vis spectrophotometer (SpectraMax Plus, Molecular Devices).

Fluorescence Spectroscopy. The fluorescence spectra for all variants were determined in 50 mM MOPS (pH 7.5) with 280 nm excitation measuring the emission in the range of 300−500 nm. Bandwidths of 10 nm for emission and excitation were used, and the scan rate was set to 100 nm/min. SYPRO Orange (SO) (catalog no. S5692, 5000× stock concentrate) was diluted 250-fold in 50 mM MOPS (pH 7.5). Protein samples were diluted to 0.3 mg/mL. Fifteen microliters of SO and protein solution was added to a final volume of 30 μL to a white 96-well MTP (Eurogentec RT-PL96-AFW), reaching a final protein concentration of 0.15 mg/mL. The plate was sealed with an optical PCR seal (Eurogentec RT-OPSL 100). Melting curves for each variant were determined (StepOnePlus Real Time PCR System, Applied Biosystems) running a temperature gradient from 25 to 96 °C at a scan rate of 76 °C/h with an initial 15 min reaction time at 25 °C. The initial relative fluorescence intensities between TlL and the variants were used to determine differences in accessible hydrophobic surface areas in aqueous solution. The fluorescence was monitored in intervals of 20 s, using LED blue light for excitation and emission detected using a Rox filter (610 nm). T_m values were calculated as the maximal value of the first derivative (dI_{fl}/dT).[30] Also, a hydrophobic surface area binding study was conducted using 8-anilinonaphthalene-1-sulfonic acid (ANS) as an extrinsic fluorophore. Crystals were dissolved in DMSO and further diluted in 50 mM MOPS (pH 7.5) to a final concentration of 1.25 mM. The final protein concentration was 0.1 mg/mL, with 0.25 mM ANS. Measurements were recorded on a fluorescence spectrometer at room temperature (PerkinElmer, LS50B) in a quartz cuvette (Hellma QS 105.250). The excitation wavelength was 380 nm with emission collected from 420 to 620 nm. Bandwidths were set to 10 nm for both excitation and emission, and the scan rate was 200 nm min^{-1}. Spectra were plotted as averages of three consecutive measurements.

RESULTS AND DISCUSSION

The aim of this study was to alter the activation mechanism of TlL to create variants with the ability to act on water-soluble substrates in the absence of an interface. To achieve this, the lid from FAEA was used as a template. One variant was also made with the entire lid domain from *A. terreus* lipase to investigate the differences between incorporating lipase and esterase lids into the TlL backbone. In this study, the lid region represents the third α-helix (residues 86−91), the anterior hinge domain (H1, residues 82−85), and the posterior hinge domain (H2, residues 92−98) when the lid is in its closed conformation (Figure 1).

Variant 1L contained the entire lid from FAEA. To investigate the effect of lid glycosylation on activity and activation, variant 2L contained an FAEA-like lid with nearly the same residue characteristics as 1L, but with the "NYTL" glycosylation site removed from the lid. Variant 3L was designed to have both TlL and FAEA character with H1 and α-helical domains resembling TlL and a H2 domain of FAEA character. The "PQ" motif at the end of H2 at positions 97 and 98 was found in many hydrolases related to FAEA (Engineering of Lid Variants) and was therefore included in the lid sequence of 3L and 3C. To create a variant with a lid locked in its open conformation, a disulfide bond was engineered into variant 3C between residues C87 and C62 within and behind the lid, respectively. Finally, the lid in variant 4L was identical to that found in AtL. Figure 2 shows the structural representations of the lid α-helix in each variant in its proposed open conformation.

Here, the α-helix represents residues 86−93 with H1 and H2 representing residues 82−85 and 94−98, respectively. For lids in TlL, 4L, 3L, and 3C, the distribution of hydrophobic amino acids in the α-helix domain is very distinct, supposedly interacting favorably with the hydrophobic active site cleft keeping the lid closed in aqueous solutions. Variants 1L and 2L have a more random distribution of hydrophobic and hydrophilic amino acids in the helical domain with polar residues pointing toward the active site cleft.

CD Spectroscopy. To compare protein folding of TlL and lid variants, far-UV CD measurements were taken to investigate secondary structure elements (Figure S3 of the Supporting

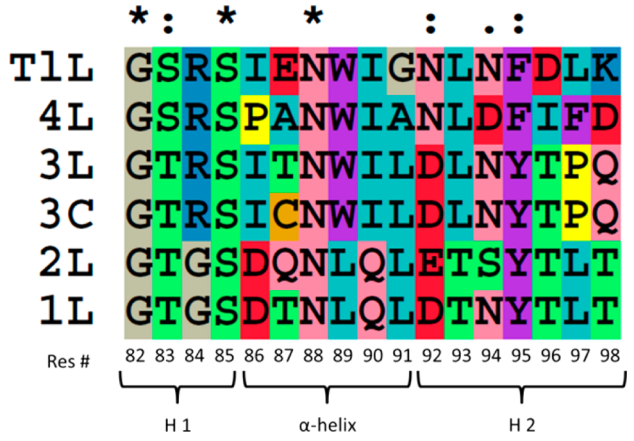

Figure 1. Multiple-sequence alignment of the lid domain of each variant in the TlL backbone spanning 17 residues from position 82 to 98. The lid domain is divided into three motifs according to the crystal structure with the lid in its closed conformation (PDB entry 1DT3[6]): residues 82−85, anterior hinge domain (H1); residues 86−91, α-helix; residues 92−98, posterior hinge domain (H2). Color code: gray for Gly, green for Ser and Thr, yellow for Pro, orange for Cys, pink for Asn and Gln, purple for Phe, Tyr, and Trp, red for Asp and Glu, blue for Arg and Lys, and cyan for Iso, Ala, and Leu. Asterisks denote a single fully conserved residue; colons denote regions of fully conserved residues that are highly similar, and the period denotes a region of conserved residues with a low degree of similarity according to the Gonnet 250 protein weight matrix. The lid alignment was created using ClustalX version 1.83.[23]

Information). The secondary structure analysis indicated that all lid variants had a structural composition similar to that of TlL in homogeneous aqueous solutions (Table S3 of the Supporting Information) with comparable fractions of α-helices, β-sheets, and turns.

Lipase Activity. Purified variants 1L, 2L, 3L, 4L, and 3C were assayed to investigate the lipase activity on medium-chain pNP-decanoate (C10) embedded in a triglyceride layer composed of triolein (Figure 3). The lipase activity was determined at pH 8, 9, and 10 (Figure 3A). Variants 1L and 2L displayed minimal levels of activity, as expected with their FAEA lid characteristics. However, the activity of variant 2L was significantly higher than that of variant 1L, demonstrating that lid glycosylation has a negative impact on activity at the lipid interface. This agrees with prior studies of lipase activity of an *A. niger* lipase variant containing the entire FAEA lid.[19] Variant 3C, with its lid locked in an open state, had low lipase activity likely explained by the enhanced rigidity of the lipase structure caused by the extra disulfide bond and hence decreased mobility at the interface. Variants 3L and 4L showed high lipase activity, with 3L displaying nearly 2-fold higher activity than 4L at all pH values. This result is somewhat surprising given that the lid in 4L is adapted from a lipase whereas the lid in 3L has both lipase and esterase character. Furthermore, variant 3L displayed activity levels that were comparable to that of TlL and significantly higher at pH 7 and 8. These results underpin the importance of the large, hydrophobic residues in the α-helix domain of the lid in maintaining activity at the interface. However, as indicated by the low activity of variant 3C, hydrophobic residues do not restore lipase activity if the lid loses flexibility. As seen from the time plot of the lipase assay, the activity of TlL and 4L displayed a "lag" phase before the activity reached its maximal value, a trait characteristic of lipases (Figure 3B).[10,32]

Interestingly, lid modifications toward a more FAEA-like character eliminated this lag phase, making the variants more quickly activated at the interface. In particular, the activation of 3L was outstanding, reaching its maximal reaction rate within 2 min compared to approximately 5 min for TlL. This enhanced rate of activation is ascribed to an altered lid residue composition supposedly lowering the activation energy of lid opening and hence decreasing the driving force needed to obtain activity at the interface. However, future MD simulations of lid opening should be conducted to confirm this. Interestingly, 3L contains an H1 domain and an α-helix domain of lipase character. Thus, it is likely the residue composition of residues in the H2 domain in 3L that is responsible for the altered activation profile.

pNP-Acetate Assay. To investigate the ability to hydrolyze water-soluble, monomeric substrates, the specific activity toward pNP-acetate was determined (Figure 4). TlL displayed the lowest degree of activity, which was comparable to the level of autohydrolysis of pNP-acetate in 50 mM Mops (pH 7.5) at 25 °C. In good agreement with the lid characteristics, variant 4L displayed nearly the same activity levels as TlL, indicating that the lid opens with a low frequency and hence is mostly closed in aqueous, monomeric solutions. The activities for variants 1L and 2L were approximately the same and significantly higher than that of TlL. However, the highest activities were displayed by 3C and 3L. For 3C, the high activity level corresponds well to the proposed disulfide bond stabilizing an open lid conformation. Interestingly, variant 3L, with a lid of esterase and lipase character, displayed activity levels significantly higher than those of 4L and TlL, indicative of a higher frequency of lid openings in aqueous solution. 3L also displayed activity levels higher than those of 1L and 2L, which could be explained by the differences in lid residues between these variants. In 1L and 2L, Trp89 has been replaced with a Leu residue. Indeed, previous studies have shown that site-directed mutagenesis of Trp89 in TlL decreases the hydrolytic activity toward an array of ester substrates ascribed to its important role in binding of the acyl chain to the active site.[33] Hence, among other possible explanations, the higher activity of 3L could be ascribed to the presence of Trp89 in the lid.

Interestingly, 3L has a distinct distribution of hydrophobic residues in the α-helix of the lid domain similar to those of TlL and 4L, which suggests a favorable interaction with the hydrophobic area around the active site keeping the lid closed in aqueous solutions. However, as these results indicate, the energy barrier of lid opening in 3L seems to be sufficiently low to allow catalysis, suggesting that the hinge domains play a key role in lid mobility. Again, H1 and the α-helix are similar among TlL, 4L, and 3L, and the observed difference in activity levels is therefore ascribed to the residue composition of the H2 domain. Previous studies of lid residue modifications of *A. niger* lipase mutants have suggested that the presence of a proline residue in the hinge domain of the lid region stabilizes an open lid conformation.[19] This is in good agreement with the presence of Pro97 in the H2 domain of 3L.

IA Assay. The hydrolytic activity as a function of pNP-butyrate concentration was determined for TlL and variants below and above the CMC according to previous procedures[9] (Figure 5). TlL and variant 4L displayed pronounced interfacial activation at the point of the CMC with a 10-fold increase in specific activity (Figure 5A). Below the CMC, activity was minimal and ascribed to a closed lid conformation, blocking

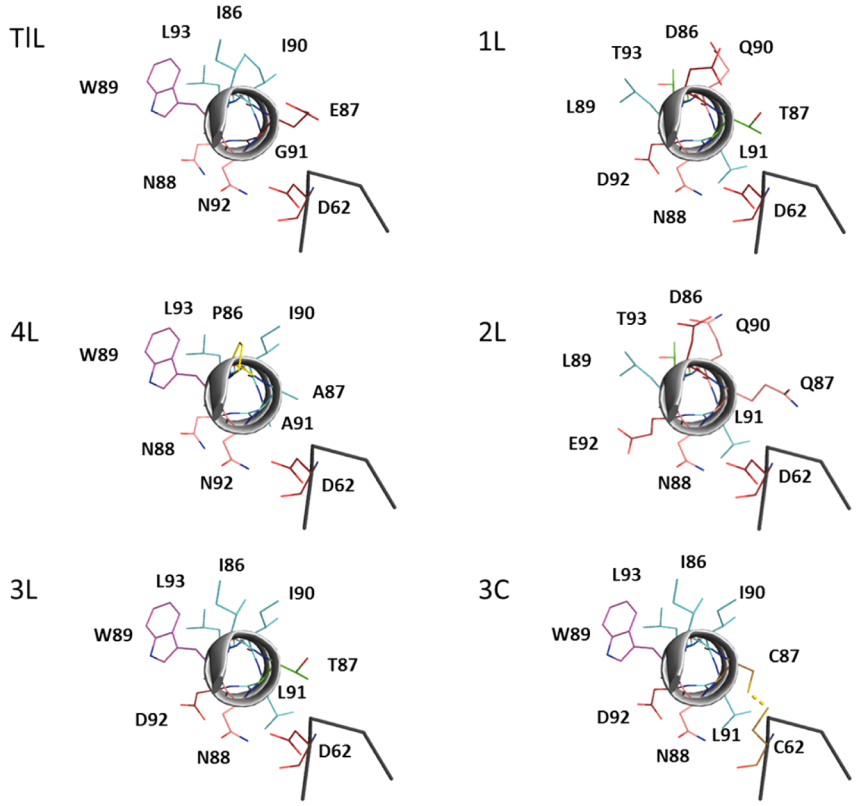

Figure 2. α-helix of the lid (positions 86–93, black lines) in TlL and lid variants presented in the open lid conformation (PDB entry 1EIN[6]) displaced from the active site. TlL, 4L, 3L, and 3C possess several large hydrophobic amino acids with a distinct distribution, whereas variants 1L and 2L contain a few, small hydrophobic residues and many polar residues in the α-helix. Amino acids are designated in one-letter code. Residue D62 in the loop (ribbon) behind the lid is also shown (black lines) with mutation D62C in variant 3C facilitating the formation of a disulfide bond, stabilizing the lid in its open state. Color code: gray for Gly, green for Thr, yellow for Pro, orange for Cys, pink for Asn and Gln, purple for Trp, red for Asp and Glu, and cyan for Iso, Ala, and Leu.[31]

access of the soluble ester substrate to the active site. However, FAEA-like lid variants 1L and 2L showed no sign of interfacial activation with activity levels significantly higher than those of 4L and TlL below the CMC (Figure 5C). Variant 3L showed pronounced interfacial activation but also showed activity below the CMC (Figure 5B). Again, this is attributed to a lower energy barrier of activation resulting in opening of the lid in the absence of an interface, agreeing well with the lipase and pNP-acetate activity results. Variant 3C displayed an FAEA-like activity profile with marked activity below the CMC with no observable interfacial activation. Notably, the activity seemed to reach a plateau as the concentration of the substrate reached approximately 0.5 mM (Figure 5B,C). This could be explained by product inhibition or formation of premicellar aggregates forming prior to the CMC. In the latter case, the aggregates would deprive the population of free, monomeric substrate molecules and hence retard the rate of hydrolysis for any variant acting on soluble esters. In either case, the reason for the observed increase in activity around 1 mM could then be explained by premicellar aggregates facilitating release of the product from the active site and thereby increasing the catalytic rate. Together, these results strongly suggest that it is the open versus closed state of the lid and the lid residue composition that determine the interfacial activation dependence in TlL.

Hydrolysis of pNP-Esters. Surfactants have been shown to affect the hydrolytic activity of TlL.[34] Hence, activity assays were conducted with pNP-butyrate and pNP-decanoate as substrates in buffers containing nonionic surfactant, Triton X-100, with and without calcium ions and EDTA (panels A and B of Figure 6, respectively).

Generally, lid variants displayed activity lower than that of TlL in calcium-rich buffers. However, for TlL, the hydrolytic activity was essentially abolished in 5 mM EDTA and 0.4% Triton X-100, whereas lid variants retained activity levels between 15 and 100%. In particular, 3C retained full activity going from conditions with calcium ions to conditions without (Figure 6C). This is likely ascribed to its open lid conformation, stabilized by a disulfide bond. Previous studies investigating the catalytic efficiency toward pNP-decanoate and palmitate have indicated that micellar concentration of Triton X-100 completely inhibits TlL activity[35] determined in buffers without calcium, which is thus in fine agreement with our presented results. Though the crystal structure of TlL does not contain a calcium binding site, these results indicate that TlL is pseudodependent on calcium ions for retaining activity in buffers containing micellar concentrations of a nonionic surfactant and that the lid region plays a central role in governing lipase activity and calcium dependency. The activity levels in this assay are approximately 100-fold higher than that obtained in the pNP-acetate and IA assay above the CMC. This dramatic increase in activity in the presence of Triton X-100 is remarkable. Previous studies have shown that addition of neutral surfactants at various submicellar and micellar concentrations increases the catalytic efficiency of lipases in solution.[34] An explanation could be that the pNP-substrate interacts with the Triton X-100 micelles to become more

dx.doi.org/10.1021/bi500233h | *Biochemistry* 2014, 53, 4152–4160

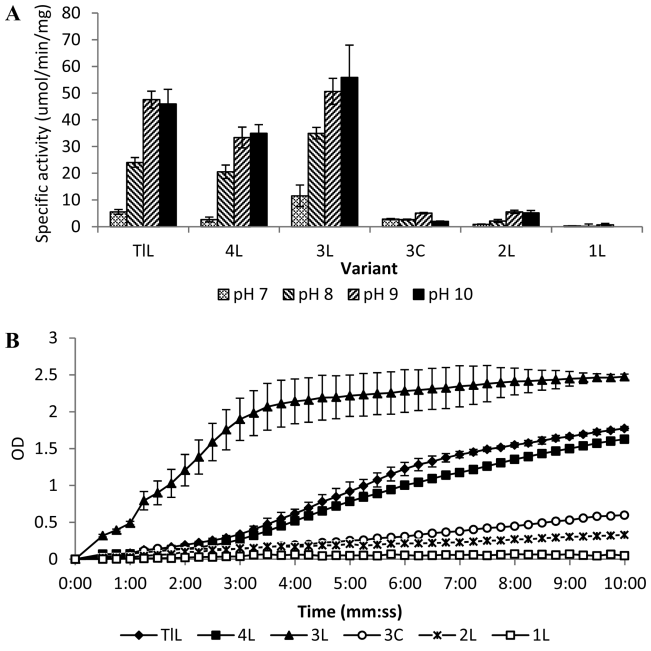

Figure 3. General lipase activity plots. The specific activity for each variant was determined on pNP-decanoate (100 nmol) embedded in a triolein layer (100 nmol). The assay was conducted in 100 mM Tris and 1 mM $CaCl_2$ (pH 7, 8, 9, and 10). The assay was conducted at 25 °C for 10 min. The specific activity was calculated from the steepest slope (A). Time plot of the optical density (OD) increase as a function of time at pH 8. The average of three absorbance measurements including the standard deviation was calculated at each time point (B). The final lipase concentration was 2 μg/mL. Error bars denote the standard deviation. Experiments were conducted in triplicate.

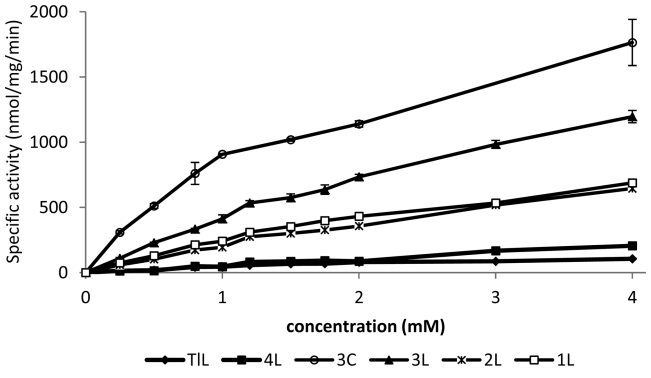

Figure 4. Specific activity of pNP-acetate as a function of concentration. Activity measured in 50 mM MOPS (pH 7.5) at 25 °C for 3 min. The final lipase concentration was ~15 μg/mL. Activity determined from the steepest slope after background subtraction. Measurements were taken in triplicate. Error bars denote the standard deviation.

accessible for the lipase. The mode of pNP-substrate−Triton X-100 interaction is not fully understood and should be investigated in the future.

Fluorescence Spectroscopy. TlL contains four tryptophan residues. Studies have shown that Trp89, located in the lid of TlL, is the main contributor to the fluorescence signal detected at 340−350 nm.[36] This is explained by the fact that the three other tryptophans are buried in the interior of the protein and have lower mobility.[37] Hence, to probe the microenvironment, the emission spectrum for each variant and

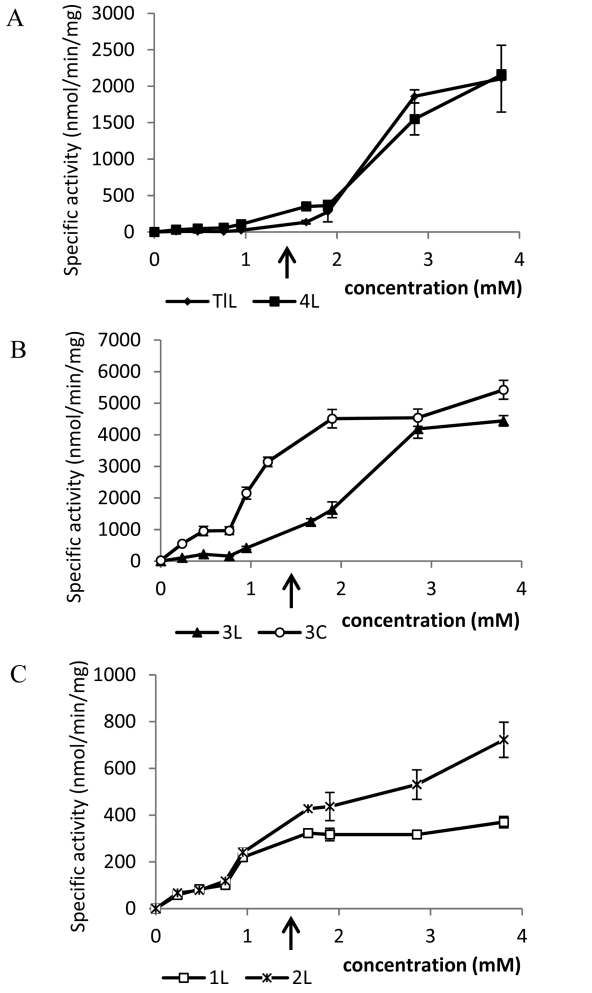

Figure 5. Interfacial activation assay showing the specific activity as a function of the concentration of pNP-butyrate in 50 mM MOPS (pH 7.5) at 25 °C. (A) Lipase constructs TlL and 4L. (B) FAEA/TlL constructs 3C and 3L. (C) FAEA constructs 1L and 2L. The black arrow denotes the point of CMC (~1.5 mM) of pNP-butyrate.[9] The final lipase concentration was ~15 μg/mL. The assay was conducted for 3 min, and the activity was determined from the steepest slope after background subtraction. Error bars denote the standard deviation. Activity was determined in triplicate.

TlL was determined (Figure S4 of the Supporting Information). TlL and 4L both displayed a single emission peak at 338 nm. For variant 3L, the profile displayed a double peak with emission maxima at 338 and 340 nm ascribed to two conformers in solution, a closed form and an open form. For variant 3C, one peak was observed at 345 nm. The red shift to longer wavelengths indicates that Trp89 in variant 3C is more exposed to the polar solvent and hence further suggests the presence of a disulfide bond that locks the lid in an open state. With no Trp89 residue, variants 1L and 2L displayed a blue-shifted emission peak at 318 nm in agreement with previous studies of a TlL Trp89Leu mutant.[38]

Melting Curve and Accessible Hydrophobic Surface Area. The stability of TlL and lid variants was determined by running a thermal melt assay measuring the fluorescence intensity from binding of SO as a function of temperature (Figure S5 of the Supporting Information). Generally, lid variants were relatively more unstable than TlL with a decrease in T_m of up to 14 °C (Table 1). Noticeably, the extra disulfide

dx.doi.org/10.1021/bi500233h | *Biochemistry* 2014, 53, 4152−4160

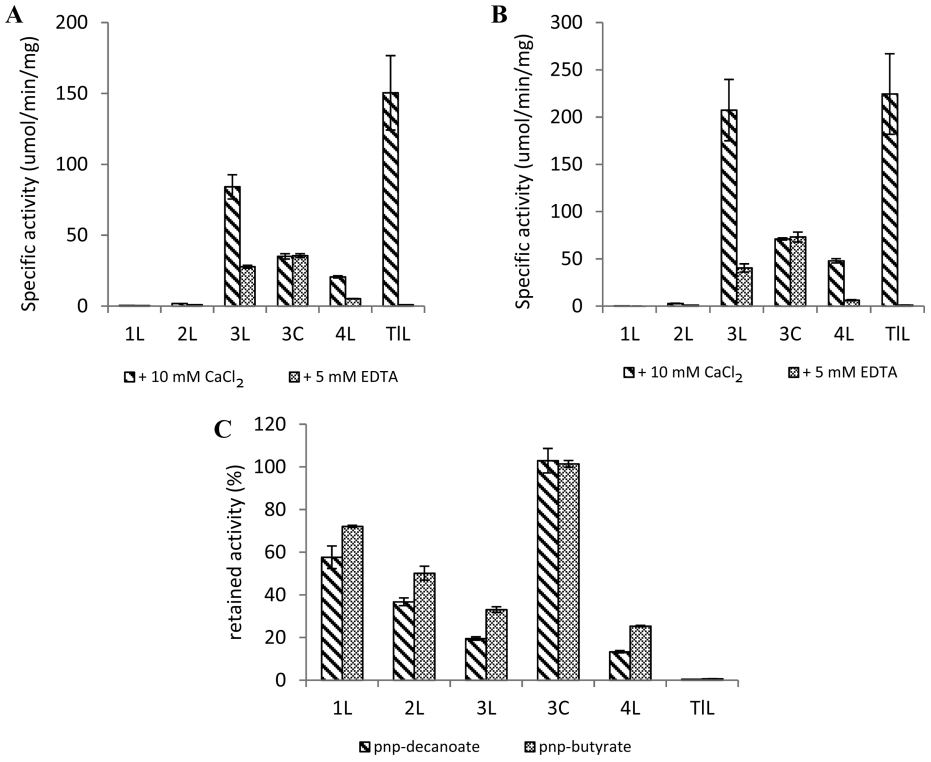

Figure 6. Specific activities of pNP-butyrate (A) and pNP-decanoate (B) determined in 50 mM Tris (pH 7.5) with 10 mM $CaCl_2$ and 5 mM EDTA, respectively. (C) Relative retained activity in buffer containing 5 mM EDTA relative to activity in buffer containing 10 mM $CaCl_2$ (pH 7.5). The gray-pattern columns show data for pNP-butyrate. The cross-hatched columns show data for pNP-decanoate. The activity was determined from the steepest slope after background subtraction. The final lipase concentration was 2 μg/mL. Measurements were taken in triplicate. Error bars denote the standard deviation.

Table 1. Spectral and Structural Properties of TlL and Lid Variants

	$\lambda_{max/280\ nm}$ [a]	T_m [b]	ANS[c]
TlL	338	72	511
4L	338	60	510
3L	338	61	492
	340		
3C	345	67	485
2L	318	59	462
1L	318	58	460

[a]Intrinsic protein fluorescence. Emission maxima determined from the average of three consecutive measurements. [b]Melting temperature determined from quadruplicate measurements, with a SD of ±0.4 °C according to previous studies.[30] [c]Emission maxima after ANS binding at room temperature. Excitation at 380 nm and emission range of 420−620 nm. Average of three consecutive measurements.

bond in 3C compared to 3L increased the melting temperature by 6 °C. To investigate the open versus closed state of the lid for each lid variant, a hydrophobic surface area binding assay was set up using SO and ANS as extrinsic fluorophores (panels A and B of Figure 7, respectively).

In the SO assay, variants 3L and 4L showed approximately the same magnitude of fluorescence as TlL whereas variants 1L, 2L, and 3C displayed 6.5−10-fold increased fluorescence intensities. These findings suggest that a large hydrophobic surface area is exposed in variants 1L, 2L, and 3C, indicating that the lid is open, which correlates with the activity assays. The SO assay was conducted on a filter-based qPCR machine, so hypso- or bathochromic shifts were not detectable. To investigate spectral shifts, the ANS assay was conducted on a monochromator-based fluorescence spectrometer. For TlL and 4L, the emission maximum was nearly the same as for ANS in buffer, around 510 nm, indicating no particular binding of ANS. For variant 3L, the emission maximum was blue-shifted to 492 nm, indicating a more hydrophobic environment for ANS. Variant 3C displayed a further blue shift to 485 nm. Interestingly, variants 1L and 2L showed the largest blue shifts of all, with peaks around 460 nm indicating a more hydrophobic and stronger binding of ANS to the protein. To make sure that the observed blue shifts are caused by hydrophobic interaction and not dominated by electrostatic contributions, future assays with neutral, positive, and negative solvent sensitive probes should be conducted.

CONCLUSION

Several studies have highlighted the lid's central role in governing substrate specificity,[39] enantioselectivity,[40] and catalytic mechanism[9] in TlL and other lipases.[18,19,41] Here, we have used a combination of activity assays and spectroscopic investigations to elucidate a correlation between the characteristics and the open versus closed state of the lid in a series of variants in aqueous solution, *in vitro*. These results indicate and support previous findings that the lid equilibrium for TlL is strongly shifted to the closed state in homogeneous aqueous solutions (Figure 8).

Via adoption of a FAEA lid residue composition, the study shows that the lid equilibrium is shifted toward an open state in aqueous solution. Variants with a FAEA-like lid adapt interfacial independence with an open lid conformation in the absence of an interface ascribed to a lowering of the activation energy of

dx.doi.org/10.1021/bi500233h | *Biochemistry* 2014, 53, 4152−4160

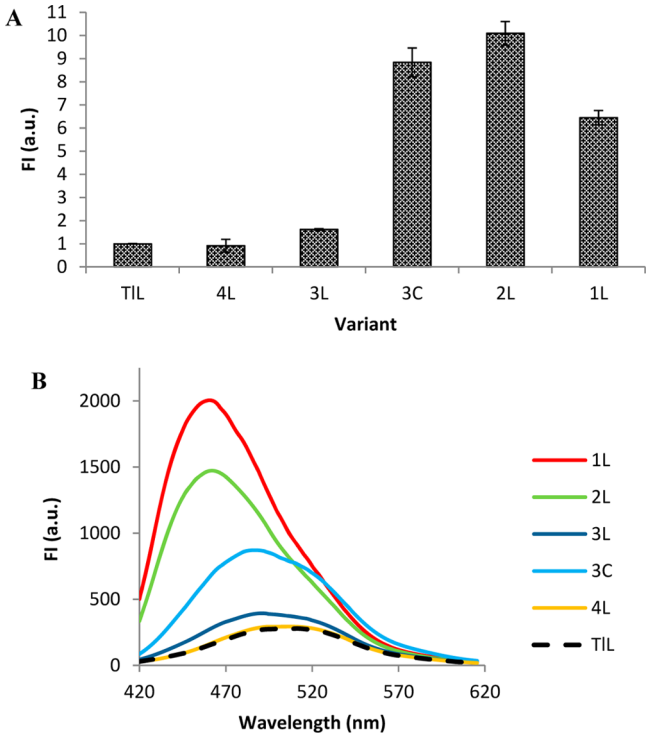

Figure 7. Accessible hydrophobic surface areas determined from binding of SYPRO Orange (SO). Protein concentrations were ~0.15 mg/mL. Values are relative to the TlL fluorescence intensity. All measurements were taken in quadruplicate. Error bars denote the propagated standard deviation (A). Fluorescence spectra of 8-anilinonaphtalene-1-sulfonic acid (ANS) binding to a hydrophobic surface area. The protein concentration was ~0.2 mg/mL. Fluorescence spectra were determined from three consecutive measurements. All measurements were taken at ambient temperature (25 °C). As ANS binds, the fluorescence intensity increases and is accompanied by a blue shift in the emission wavelength maximum (B).

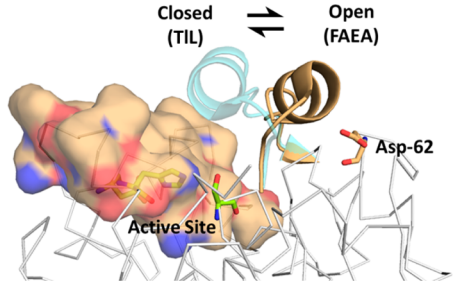

Figure 8. Closed lid (PDB entry 1DT3, cyan) and open lid (PDB entry 1EIN, orange cartoon representation) in the *T. lanuginosus* lipase backbone (white ribbon). As proposed from the presented results, the TlL lid equilibrium (black arrows) is strongly shifted to the closed state in homogeneous aqueous solutions. As the lid adapts characteristics of FAEA, the lid equilibrium is shifted to the open state. Upon opening, the lid moves away from the active site, exposing a large hydrophobic patch (orange surface), rendering the active site accessible for the substrate. The catalytic triad is shown as green sticks. Residue Asp62 (orange sticks) is highlighted behind the lid.[31]

lid opening. However, these variants were nearly inactive at the water–lipid surface and thus lost lipase activity. To the best of our knowledge, this work presents the first examples of lipase variants with mutations spanning the entire lid region (H1, H2, and α-helix) that contain residues from FAEA and related hydrolases. This approach has facilitated the generation of TlL variants with intermediate lids of both esterase and lipase character. Interestingly, these results reveal that it is possible to embrace functionality from both worlds to make lipase variants with high lipase activity, fast activation at the lipid interface, and an ability to act on water-soluble substrates, including an enhanced degree of calcium independence.

■ ASSOCIATED CONTENT

Supporting Information

An alignment of the FAEA-related hydrolases from the PSI search containing the "PQ" motif in the H2 domain of the lid region at positions 97 and 98 (TlL numbering), a table of the primers used to generate the lid variants, a table showing the calculated and observed molecular weights of each lid variant and TlL determined by LC-ESI-TOF MS, an alignment of the entire primary sequences of the TlL and lid variants presented in this study, CD spectra and table showing secondary structural elements of TlL and lid variants, a figure showing the fluorescence spectra of TlL and lid variants, and figures showing the fluorescence intensity as a function of temperature for TlL and lid variants in the thermal melt assay using SYPRO Orange. This material is available free of charge via the Internet at http://pubs.acs.org.

■ AUTHOR INFORMATION

Corresponding Author

*Universitetsparken 5, 2100 København Ø, Denmark. Telephone: +45 29 26 04 52. E-mail: mobj@chem.ku.dk.

Funding

This work was funded by the industrial Ph.D. program EFU:Novozymes (12-128740 and 0604-01457B).

Notes

The authors declare no competing financial interest.

■ ACKNOWLEDGMENTS

We thank the researchers at Novozymes R&D for assistance. Special thanks to Clive P. Walter, Christian I. Jørgensen, Maria B. Silow, Vikram K. Bhatia, and Frank W. Rasmussen for technical assistance.

■ ABBREVIATIONS

CMC, critical micelle concentration; TlL, *T. lanuginosus* lipase; AtL, *A. terreus* lipase; FAEA, *A. niger* ferulic acid esterase; pNP, *p*-nitrophenol.

■ REFERENCES

(1) Schmid, R. D., and Verger, R. (1998) Lipases: Interfacial Enzymes with Attractive Applications. *Angew. Chem., Int. Ed. 37*, 1608–1633.

(2) Derewenda, U., Swenson, L., Wei, Y., Green, R., Kobos, P. M., Joerger, R., Haas, M. J., and Derewenda, Z. S. (1994) Conformational lability of lipases observed in the absence of an oil-water interface: Crystallographic studies of enzymes from the fungi *Humicola lanuginosa* and *Rhizopus delemar*. *J. Lipid Res. 35*, 524–534.

(3) Ollis, D. L., Cheah, E., Cygler, M., Dijkstra, B., Frolow, F., Franken, S. M., Harel, M., Remington, S. J., Silman, I., Schrag, J., et al. (1992) The α/β hydrolase fold. *Protein Eng. 5*, 197–211.

(4) Boel, E., Christensen, T., and Woeldike, H. F. (2009) Process for the production of protein products in *Aspergillus*. NOVO NORDISK A/S. Patent 08435557[7517668].

(5) Peters, G. H., Svendsen, A., Langberg, H., Vind, J., Patkar, S. A., and Kinnunen, P. K. J. (2002) Glycosylation of *Thermomyces lanuginosa* lipase enhances surface binding towards phospholipids,

but does not significantly influence the catalytic activity. *Colloids Surf., B 26*, 125−134.
(6) Brzozowski, A. M., Savage, H., Verma, C. S., Turkenburg, J. P., Lawson, D. M., Svendsen, A., and Patkar, S. (2000) Structural Origins of the Interfacial Activation in *Thermomyces* (*Humicola*) *lanuginosa* Lipase. *Biochemistry 39*, 15071−15082.
(7) Brzozowski, A. M., Derewenda, U., Derewenda, Z. S., Dodson, G. G., Lawson, D. M., Turkenburg, J. P., Bjorkling, F., Huge-Jensen, B., Patkar, S. A., and Thim, L. (1991) A model for interfacial activation in lipases from the structure of a fungal lipase-inhibitor complex. *Nature 351*, 491−494.
(8) Sarda, L., and Desnuelle, P. (1958) Action de la lipase pancrèatique sur les esters en èmulsion. *Biochim. Biophys. Acta 30*, 513−521.
(9) Martinelle, M., Holmquist, M., and Hult, K. (1995) On the interfacial activation of *Candida antarctica* lipase A and B as compared with *Humicola lanuginosa* lipase. *Biochim. Biophys. Acta 1258*, 272−276.
(10) Louwrier, A., Drtina, G. J., and Klibanov, A. M. (1996) On the issue of interfacial activation of lipase in nonaqueous media. *Biotechnol. Bioeng. 50*, 1−5.
(11) Santini, S., Crowet, J. M., Thomas, A., Paquot, M., Vandenbol, M., Thonart, P., Wathelet, J. P., Blecker, C., Lognay, G., Brasseur, R., Lins, L., and Charloteaux, B. (2009) Study of *Thermomyces lanuginosa* Lipase in the Presence of Tributyrylglycerol and Water. *Biophys. J. 96*, 4814−4825.
(12) Peters, G. H., Toxvaerd, S., Olsen, O. H., and Svendsen, A. (1997) Computational studies of the activation of lipases and the effect of a hydrophobic environment. *Protein Eng. 10*, 137−147.
(13) Rehm, S., Trodler, P., and Pleiss, J. (2010) Solvent-induced lid opening in lipases: A molecular dynamics study. *Protein Sci. 19*, 2122−2130.
(14) Svendsen, A. (2000) Lipase protein engineering. *Biochim. Biophys. Acta 1543*, 223−238.
(15) McAuley, K. E., Svendsen, A., Patkar, S. A., and Wilson, K. S. (2004) Structure of a feruloyl esterase from *Aspergillus niger*. *Acta Crystallogr. D60*, 878−887.
(16) Neves Petersen, M. T., Fojan, P., and Petersen, S. B. (2001) How do lipases and esterases work: The electrostatic contribution. *J. Biotechnol. 85*, 115−147.
(17) Aliwan, F. O., Kroon, P. A., Faulds, C. B., Pickersgill, R., and Williamson, G. (1999) Ferulic acid esterase-III from *Aspergillus niger* does not exhibit lipase activity. *J. Sci. Food Agric. 79*, 457−459.
(18) Shu, Z., Duan, M., Yang, J., Xu, L., and Yan, Y. (2009) *Aspergillus niger* lipase: Heterologous expression in *Pichia pastoris*, molecular modeling prediction and the importance of the hinge domains at both sides of the lid domain to interfacial activation. *Biotechnol. Prog. 25*, 409−416.
(19) Shu, Z., Wu, J., Xue, L., Lin, R., Jiang, Y., Tang, L., Li, X., and Huang, J. (2011) Construction of *Aspergillus niger* lipase mutants with oil−water interface independence. *Enzyme Microb. Technol. 48*, 129−133.
(20) Yu, X. W., Zhu, S. S., Xiao, R., and Xu, Y. (2014) Conversion of a *Rhizopus chinensis* Lipase into an Esterase by Lid Swapping. *J. Lipid Res. 55*, 1044−1051.
(21) Goujon, M., McWilliam, H., Li, W., Valentin, F., Squizzato, S., Paern, J., and Lopez, R. (2010) A new bioinformatics analysis tools framework at EMBL−EBI. *Nucleic Acids Res. 38*, W695−W699.
(22) Edgar, R. C. (2004) MUSCLE: Multiple sequence alignment with high accuracy and high throughput. *Nucleic Acids Res. 32*, 1792−1797.
(23) Larkin, M. A., Blackshields, G., Brown, N. P., Chenna, R., McGettigan, P. A., McWilliam, H., Valentin, F., Wallace, I. M., Wilm, A., Lopez, R., Thompson, J. D., Gibson, T. J., and Higgins, D. G. (2007) Clustal W and Clustal X version 2.0. *Bioinformatics 23*, 2947−2948.
(24) Ho, S. N., Hunt, H. D., Horton, R. M., Pullen, J. K., and Pease, L. R. (1989) Site-directed mutagenesis by overlap extension using the polymerase chain reaction. *Gene 77*, 51−59.
(25) Christensen, T., Woeldike, H., Boel, E., Mortensen, S. B., Hjortshoej, K., Thim, L., and Hansen, M. T. (1988) High Level Expression of Recombinant Genes in *Aspergillus oryzae*. *Nat. Biotechnol. 6*, 1419−1422.
(26) Vind, J. (1999) Constructing and screening a DNA library of interest in filamentous fungal cells. WO200024883.
(27) Hedin, E. M., Patkar, S. A., Vind, J., Svendsen, A., Hult, K., and Berglund, P. (2002) Selective reduction and chemical modification of oxidized lipase cysteine mutants. *Can. J. Chem. 80*, 529−539.
(28) Lobley, A., Whitmore, L., and Wallace, B. A. (2002) DICHROWEB: An interactive website for the analysis of protein secondary structure from circular dichroism spectra. *Bioinformatics 18*, 211−212.
(29) Compton, L. A., and Johnson, W. C., Jr. (1986) Analysis of protein circular dichroism spectra for secondary structure using a simple matrix multiplication. *Anal. Biochem. 155*, 155−167.
(30) Crowther, G. J., Napuli, A. J., Thomas, A. P., Chung, D. J., Kovzun, K. V., Leibly, D. J., Castaneda, L. J., Bhandari, J., Damman, C. J., Hui, R., Hol, W. G. J., Buckner, F. S., Verlinde, C. L. M. J., Zhang, Z., Fan, E., and van Voorhis, W. C. (2009) Buffer Optimization of Thermal Melt Assays of Plasmodium Proteins for Detection of Small-Molecule Ligands. *J. Biomol. Screening 14*, 700−707.
(31) DeLano, W. L. (2002) *PyMOL Molecular Graphics System*, DeLano Scientific, San Carlos, CA.
(32) Chahinian, H., Nini, L., Boitard, E., Dubés, J. P., Comeau, L. C., and Sarda, L. (2002) Distinction between esterases and lipases: A kinetic study with vinyl esters and TAG. *Lipids 37*, 653−662.
(33) Martinelle, M., Holmquist, M., Clausen, I. G., Patkar, S., Svendsen, A., and Hult, K. (1996) The role of Glu87 and Trp89 in the lid of *Humicola lanuginosa* lipase. *Protein Eng. 9*, 519−524.
(34) Mogensen, J. E., Sehgal, P., and Otzen, D. E. (2005) Activation, Inhibition, and Destabilization of *Thermomyces lanuginosus* Lipase by Detergents. *Biochemistry 44*, 1719−1730.
(35) Palacios, D., Busto, M. D., and Ortega, N. (2014) Study of a new spectrophotometric end-point assay for lipase activity determination in aqueous media. *LWT—Food Sci. Technol. 55*, 536−542.
(36) Stobiecka, A., Wysocki, S., and Brzozowski, A. M. (1998) Fluorescence study of fungal lipase from *Humicola lanuginosa*. *J. Photochem. Photobiol., B 45*, 95−102.
(37) Cajal, Y., Svendsen, A., De Bolos, J., Patkar, S. A., and Alsina, M. A. (2000) Effect of the lipid interface on the catalytic activity and spectroscopic properties of a fungal lipase. *Biochimie 82*, 1053−1061.
(38) Jutila, A., Zhu, K., Tuominen, E. K. J., and Kinnunen, P. K. J. (2004) Fluorescence spectroscopic characterization of *Humicola lanuginosa* lipase dissolved in its substrate. *Biochim. Biophys. Acta 1702*, 181−189.
(39) Holmquist, M., Martinelle, M., Clausen, I. G., Patkar, S., Svendsen, A., and Hult, K. (1994) Trp89 in the lid of *Humicola lanuginosa* lipase is important for efficient hydrolysis of tributyrin. *Lipids 29*, 599−603.
(40) Overbeeke, P. L., Govardhan, C., Khalaf, N., Jongejan, J. A., and Heijnen, J. J. (2000) Influence of lid conformation on lipase enantioselectivity. *J. Mol. Catal. B: Enzym. 10*, 385−393.
(41) Secundo, F., Carrea, G., Tarabiono, C., Gatti-Lafranconi, P., Brocca, S., Lotti, M., Jaeger, K. E., Puls, M., and Eggert, T. (2006) The lid is a structural and functional determinant of lipase activity and selectivity. *J. Mol. Catal. B: Enzym. 39*, 166−170.